American Mineralogist, Volume 93, pages 698–701, 2008

LETTER

Crystal structure and Raman spectrum of hydroxyl-bästnasite-(Ce), $CeCO_3(OH)$

HEXIONG YANG,[1,*] ROBERT F. DEMBOWSKI,[1] PAMELA G. CONRAD,[2] AND ROBERT T. DOWNS[1]

[1]Department of Geosciences, University of Arizona, Tucson, Arizona 85721-0077, U.S.A.
[2]Jet Propulsion Laboratory, MS-183-301, 4800 Oak Grove Drive, Pasadena, California 91109-8099, U.S.A.

ABSTRACT

Hydroxyl-bästnasite-(Ce), ideally $CeCO_3(OH)$, had been regarded isostructural with bästnasite-(Ce), $CeCO_3F$, the dominant member of the bästnasite family that produces ~70% of the world's supply of rare-earth elements. Using single-crystal X-ray diffraction and Raman spectroscopy, our structural analysis on hydroxyl-bästnasite-(Ce) shows that the previous assumption is incorrect. The crystal structure of hydroxyl-bästnasite-(Ce) possesses $P\bar{6}$ symmetry with unit-cell parameters a = 12.4112(2), c = 9.8511(3) Å, and V = 1314.2(1) Å^3, in contrast to the space group $P\bar{6}2c$ and $a \approx 7.10$, $c \approx 9.76$ Å, and $V \approx 430$ Å^3 for bästnasite-(Ce). Moreover, there are 6, 3, and 5 symmetrically-distinct CO_3 groups, Ce cations, and (OH/F) ions, respectively, in hydroxyl-bästnasite-(Ce), but 1, 1, and 2 in bästnasite-(Ce). The two structures, nevertheless, are similarly characterized by the layers of CO_3 groups alternating with the Ce-(OH/F) layers along the ***c*** direction. The Raman spectrum of hydroxyl-bästnasite-(Ce) is dominated by three strong bands at 1080, 1087, and 1098 cm^{-1} in the CO_3 symmetrical stretching region, along with at least four bands in the OH stretching region. Our study further suggests that natural hydroxyl-bästnasite-(Nd) is most likely isotypic with hydroxyl-bästnasite-(Ce), rather than with bästnasite-(Ce), as previously proposed.

Keywords: Bästnasite, hydroxyl-bästnasite-(Ce), single-crystal X-ray diffraction, crystal structure, Raman spectra

INTRODUCTION

Recent developments in high-technology industries, such as laser materials, high-power magnetic materials, and ionic conductors, have generated a tremendous demand for rare earth elements (REE) (Bünzli et al. 2007 and references therein). Among all REE-bearing mineral resources in the world, bästnasite, $(REE)CO_3F$, is the most abundant, and about 70% of REE products come from bästnasite production (Chi et al. 2004). The crystal structure of bästnasite-(Ce) was first proposed by Oftedal (1931) and confirmed by Donnay and Donnay (1953) on the basis of X-ray photographic data. More detailed structure analyses on this mineral, however, were not conducted until the 1990s (Ni et al. 1993; Terada et al. 1993; Mi et al. 1996). The structure of bästnasite-(Ce), hexagonal with space group $P\bar{6}2c$, consists of (001) layers of CO_3 groups sandwiched by Ce-F sheets. Notably, many REE-bearing fluorcarbonate minerals, such as parisite $CaCe_2(CO_3)_3F_2$, röntgenite-(Ce) $Ca_2Ce_3(CO_3)_5F_3$, and synchysite-(Ce) $CaCe(CO_3)_2F$, contain the bästnasite structure as a basic building module (Ni et al. 1993, 2000).

Hydroxyl-bästnasite-(Ce), ideally $CeCO_3(OH)$, was first described as a new variety and the OH-analog of bästnasite-(Ce) by Kirillov (1964) and later by Minakawa et al. (1992). Maksimović and Pantó (1985) reported hydroxyl-bästnasite-(Nd). Based on the strong similarities in powder X-ray diffraction patterns and crystal chemistry, all previous studies assumed that hydroxyl-bästnasite and bästnasite were isotypic. In this paper, we report the first structural investigation of hydroxyl-bästnasite-(Ce) using single-crystal X-ray diffraction and Raman spectroscopy and demonstrate that this mineral is not isomorphous with bästnasite-(Ce).

EXPERIMENTAL METHODS

The hydroxyl-bästnasite-(Ce) specimen used in this study is from Trimouns, Luzenac, France and is in the collection of the RRUFF project (deposition no. R060283; http://rruff.info), donated by Herb Obodda. The chemical composition was determined with a CAMECA SX50 electron microprobe (http://rruff.info). The OH content was estimated based on the charge balance and the CO_3 content was calculated from the difference off 100 wt%. The average composition (12 point analyses), normalized to CO_3 = 1.0, yielded a formula of $(Ce_{0.50}Nd_{0.24}La_{0.23}Y_{0.03})_{\Sigma=1}CO_3[(OH)_{0.65}F_{0.35}]_{\Sigma=1}$.

Based on optical examination and X-ray diffraction peak profiles, a nearly equidimensional crystal was selected and mounted on a Bruker X8 APEX2 CCD X-ray diffractometer equipped with graphite-monochromatized Mo$K\alpha$ radiation. X-ray diffraction data were collected with frame widths of 0.5° in ω and 30 s counting time per frame. All reflections were indexed on the basis of a hexagonal unit-cell (Table 1). The intensity data were corrected for X-ray absorption using the Bruker program SADABS. The lack of systematic absences of reflections is consistent with the space group $P6$, $P\bar{6}$, or $P6/m$. The crystal structure was solved and refined with space group $P\bar{6}$ using the direct methods (SHELX97) (Sheldrick 1997), because only this space group gave the reasonable refinement statistics (bond lengths and angles, atomic displacement parameters, and R factors). In the structure refinement, the REE sites were assumed to be fully occupied by Ce, as the average atomic number of $(Ce_{0.50}Nd_{0.24}La_{0.23}Y_{0.03})$ is close to that of Ce. The chemical analysis showed the presence of F^- substituting for OH^-, but the final refinement assumed that all OH sites were occupied by O only. The positions of all atoms were refined with anisotropic displacement parameters, except for H atoms, which were not located by the difference Fourier syntheses. Final coordinates and displacement parameters of non-H atoms are listed in Table 2, and selected bond-distances in Table 3.

Raman spectra of the sample were collected from a randomly oriented crystal

* E-mail: hyang@u.arizona.edu

TABLE 1. Summary of crystal data and refinement results for hydroxyl-bästnasite-(Ce)

Structural formula	$(Ce_{0.50}Nd_{0.24}La_{0.23}Y_{0.03})_{\Sigma=1}CO_3[(OH)_{0.65}F_{0.35}]_{\Sigma=1}$
Crystal size (mm)	0.06 × 0.06 × 0.06
Space group	$P\bar{6}$ (No. 174)
a (Å)	12.4112(2)
c (Å)	9.8511(3)
V (Å³)	1314.2(1)
Z	18
ρ_{calc} (g/cm³)	4.936
λ (Å)	0.71069
μ (mm⁻¹)	15.84
θ range for data collection	2.07 to 34.02
No. of reflections collected	23310
No. of independent reflections	3742
No. of reflections with $I > 2\sigma(I)$	3262
No. of parameters refined	183
R(int)	0.043
Final *R* factors [$I > 2\sigma(I)$]	$R_1 = 0.028$, $wR_2 = 0.067$
Final *R* factors (all data)	$R_1 = 0.035$, $wR_2 = 0.072$
Goodness-of-fit	1.069

TABLE 2. Atomic coordinates and isotropic displacement parameters for hydroxyl-bästnasite-(Ce)

Atom	*x*	*y*	*z*	U_{eq} (Å²)
Ce1	0.1099(1)	0.2290(1)	0.2395(1)	0.0075(1)
Ce2	0.4385(1)	0.2171(1)	0.2555(1)	0.0087(1)
Ce3	0.1050(1)	0.5591(1)	0.2590(1)	0.0077(1)
C1	0.4896(7)	0.3571(7)	0	0.019(1)
C2	0.2012(6)	0.0893(6)	0	0.010(1)
C3	0.3015(7)	0.4669(8)	0	0.022(2)
C4	0.5518(6)	0.4178(7)	½	0.013(1)
C5	0.2397(6)	0.4656(6)	½	0.011(1)
C6	0.2028(6)	0.0255(6)	½	0.010(1)
O1	0.4887(6)	0.2479(6)	0	0.025(1)
O2	0.4924(4)	0.4052(3)	0.1139(3)	0.014(1)
O3	0.0288(4)	0.1690(5)	0	0.014(1)
O4	0.2341(3)	0.1490(3)	0.1136(3)	0.010(1)
O5	0.1619(6)	0.5875(6)	0	0.029(2)
O6	0.2515(3)	0.4195(3)	0.1130(3)	0.016(1)
O7	0.4997(5)	0.2993(5)	½	0.014(1)
O8	0.5185(4)	0.0962(3)	0.3865(4)	0.012(1)
O9	0.3596(5)	0.5242(5)	½	0.013(1)
O10	0.1787(3)	0.4333(3)	0.3863(3)	0.010(1)
O11	0.0819(5)	0.1799(5)	½	0.012(1)
O12	0.2511(3)	0.0738(3)	0.3868(3)	0.010(1)
OH1	0	0	0.2681(6)	0.019(1)
OH2	2/3	1/3	0.2375(7)	0.022(1)
OH3	1/3	2/3	0.2377(6)	0.018(1)
OH4	0.3226(3)	0.3212(3)	0.3217(3)	0.018(1)
OH5	0.3438(3)	0.0002(3)	0.1793(3)	0.018(1)

at 100% power on a Thermo Almega microRaman system, using a solid-state laser with a frequency of 532 nm and a thermoelectric cooled CCD detector. The laser is partially polarized with 4 cm⁻¹ resolution and a spot size of 1 μm. For comparison, the Raman spectrum for a bästnasite-(Ce) sample from our RRUFF project collection (R060359) was also reported here.

RESULTS AND DISCUSSION

Hydroxyl-bästnasite-(Ce) is found to be isostructural with the synthetic compounds $NdCO_3(OH)$ (Christensen 1973) and $Dy(CO_3)(OH)$ (Kutlu and Meyer 1999), rather than with bästnasite-(Ce) (Ni et al. 1993; Terada et al. 1993; Mi et al. 1996), which has space group $P\bar{6}2c$ and unit-cell parameters $a_{bästnasite} \approx a/\sqrt{3}$, $c_{bästnasite} \approx c$, and $V_{bästnasite} \approx V/3$, where *a*, *c*, and *V* are the unit-cell parameters for hydroxyl-bästnasite-(Ce). The crystal structure of hydroxyl-bästnasite-(Ce), nevertheless, exhibits many features similar to that of bästnasite-(Ce). For example, both structures are composed of layers of CO_3 groups alternating with the Ce-(OH/F) layers in the ***c*** direction (Fig. 1). In the CO_3 layers, two of three O atoms within a CO_3 group are superimposed upon each other in the *c* direction, whereas the third O atom and the C atom are situated on the mirror planes perpendicular to the ***c*** axis. Moreover, all Ce cations in both structures are bonded by nine ions: three (OH/F) ions in the same layer and six O ions from the CO_3 layers. The principal difference between the two structures are that there are 6, 3, and 5 symmetrically-independent CO_3 groups, Ce cations, and (OH/F) ions, respectively, in hydroxyl-bästnasite-(Ce), but 1, 1, and 2 in bästnasite-(Ce). The average C-O distances of 1.28–1.30 Å in hydroxyl-bästnasite-(Ce) match those observed in bästnasite-(Ce) (Ni et al. 1993; Terada et al. 1993; Mi et al. 1996), synthetic $NdCO_3(OH)$ (Christensen 1973), and $DyCO_3(OH)$ (Kutlu and Meyer 1999). However, the average Ce-(OH/F) and Ce-O bond lengths in hydroxyl-bästnasite-(Ce), which are ~2.460(3) and 2.551(3) Å, respectively, are significantly different from the corresponding ones in bästnasite-(Ce) [2.407(2) and 2.571(5) Å, respectively].

TABLE 3. Selected interatomic distances (Å) in hydroxyl-bästnasite-(Ce)

	Distance		Distance
Ce1-O3	2.527(2)	C1-O1	1.350(9)
Ce1-O4	2.535(3)	C1-O2 (×2)	1.263(5)
Ce1-O6	2.466(3)	Average	1.292
Ce1-O10	2.662(3)		
Ce1-O11	2.620(1)		
Ce1-O12	2.501(3)		
Ce1-OH1	2.478(1)	C2-O3	1.270(8)
Ce1-OH4	2.431(3)	C2-O4 (×2)	1.291(5)
Ce1-OH5	2.488(3)	Average	1.284
Average	2.523		
Ce2-O1	2.575(2)	C3-O5	1.357(9)
Ce2-O2	2.506(3)	C3-O6 (×2)	1.267(5)
Ce2-O4	2.638(3)	Average	1.297
Ce2-O7	2.577(2)		
Ce2-O8	2.529(3)		
Ce2-O12	2.472(3)		
Ce2-OH2	2.459(1)	C4-O7	1.277(9)
Ce2-OH4	2.455(3)	C4-O8 (×2)	1.313(5)
Ce2-OH5	2.456(3)	Average	1.301
Average	2.519		
Ce3-O2	2.566(3)	C5-O9	1.289(9)
Ce3-O5	2.614(2)	C5-O10 (×2)	1.298(5)
Ce3-O6	2.518(4)	Average	1.295
Ce3-O8	2.546(3)		
Ce3-O9	2.551(2)		
Ce3-O10	2.510(3)		
Ce3-OH3	2.464(1)	C6-O11	1.317(8)
Ce3-OH4	2.497(3)	C6-O12 (×2)	1.266(4)
Ce3-OH5	2.442(3)	Average	1.283
Average	2.523		

The structural differences between hydroxyl-bästnasite-(Ce) and bästnasite-(Ce) are also manifest in their Raman spectra (Fig. 2). Specifically, the Raman spectrum of bästnasite-(Ce) is dominated by a strong, narrow band at 1096 cm⁻¹ that can be assigned to the CO_3 symmetrical stretching vibrations and there are no significant bands in the region between 3200 and 3700 cm⁻¹. In contrast, the Raman spectrum of hydroxyl-bästnasite-(Ce) displays three strong bands at 1080, 1087, and 1098 cm⁻¹ in the CO_3 symmetrical stretching region, along with at least four bands in the OH stretching region. The observation of three discrete CO_3 symmetrical stretching bands, instead of one, indicates that there may be at least three structurally-nonequivalent CO_3 groups in the hydroxyl-bästnasite-(Ce) structure, consistent with

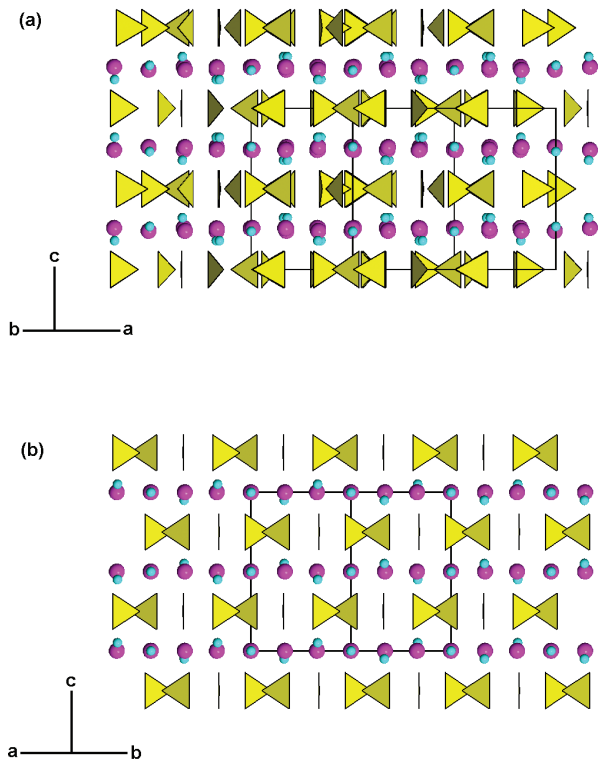

FIGURE 1. Comparison of crystal structures of (**a**) hydroxyl-bästnasite-(Ce) viewed along [120] and (**b**) bästnasite-(Ce) viewed along [110]. Yellow triangles, large purple, and small light-blue spheres represent CO_3 groups, F, and Ce atoms, respectively.

our structure refinement data.

Although our structure refinement did not locate the positions of H atoms in hydroxyl-bästnasite-(Ce) owing to the presence of the heavy REE, the four bands in the OH stretching region point to the possible existence of at least four distinct O-H bonding environments in the structure. According to Nakamoto et al. (1955), Novak (1974), and Libowitzky (1999), the Raman bands we observed at 3235, 3493, 3568, and 3638 cm^{-1} would correspond to the O-H···O distances of ~2.72, ~2.85, 2.95–3.00, and 3.2–3.3 Å, respectively. These values can all be found around the five OH sites in the hydroxyl-bästnasite-(Ce) structure. In fact, 30 O atoms in total are at distances between 2.719 and 3.239 Å from the five OH ions, which makes it difficult for us to resolve which individual O···O pairs are probably H-bonded.

Between the two symmetrically distinct F atoms in bästnasite-(Ce), the F1 atom, which is situated at the 2*a* position (site symmetry 32), shows longer separations to the three bonded Ce atoms and six nearest neighboring O atoms than the F2 atom at the 4*f* position (site symmetry 3) (Ni et al. 1993; Terada et al. 1993; Mi et al. 1996). Thus, the F1 atom is less closely-packed and would be energetically more favorable for OH substitution than the F2 site. Similarly, the OH sites with higher site symmetry in hydroxyl-bästnasite-(Ce), namely OH1, OH2, and OH3, are also less closely-packed than those (OH4 and OH5) with lower site symmetry. By the same token, we may expect some enrichment of F in the OH4 and OH5 sites in our sample, as it contains a considerable amount of F. The bond-valence sums (Brown 1996) for the five OH sites, calculated by assuming that they are all solely occupied by O atoms, however, did not yield much useful information about the possible F-OH ordering in our sample, as they all fall between 1.24 and 1.30 v.u. Note that a consideration of the substitution of some F for OH will reduce these values close to one, lending support to our chemical analysis results.

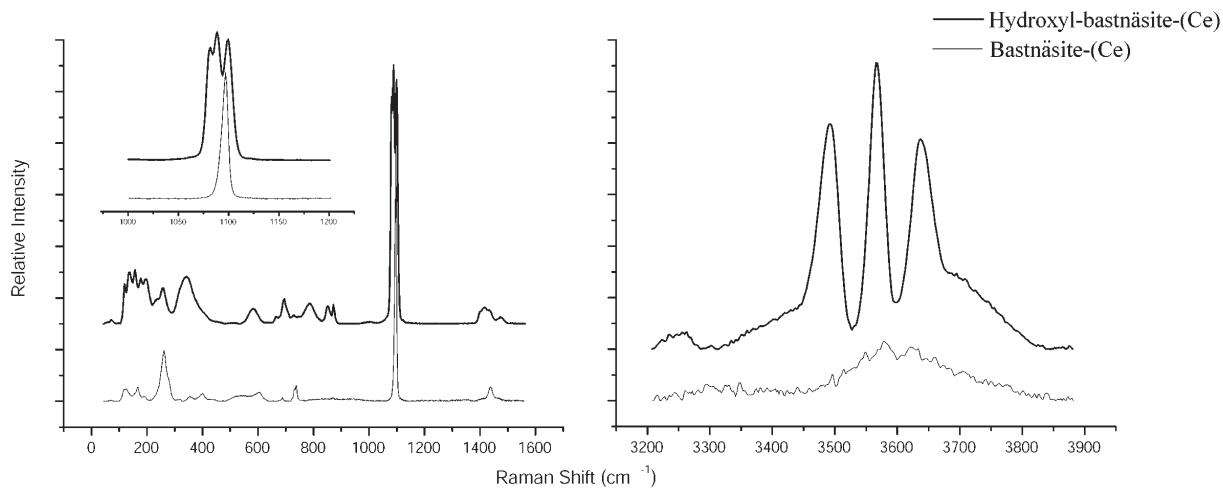

FIGURE 2. Raman spectra of hydroxyl-bästnasite-(Ce) and bästnasite-(Ce). The band assignments are as follows: between 1000–1200 cm^{-1} = ν_1 CO_3 symmetric al stretching modes; between 1300–1500 cm^{-1} = ν_3 CO_3 anti-symmetrical stretching modes; between 530–930 cm^{-1} = ν_2 and ν_4 CO_3 in-plane and out-of-plane bending modes; below 500 cm^{-1} = hydroxyl deformation modes, Ce-(OH/F) stretching vibrations, and lattice modes; between 3200–3800 cm^{-1} = OH stretching vibrations.

There have been considerable discussions about the effects of the F-OH substitution on crystal structures and properties of minerals (Groat et al. 1990; Cooper and Hawthorne 1995; Yang et al. 2007a, 2007b). For some minerals, the OH- and F-members form a continuous solid solution, such as for the amblygonite [$LiAl(PO_4)F$]-montebrasite [$LiAl(PO_4)(OH)$] and fluorapatite [$Ca_5(PO_4)_3F$]-hydroxylapatite [$Ca_5(PO_4)_3(OH)$] series. However, there are also many examples in which the F-OH substitution results in structural transformations or symmetry changes, such as the cases between $C2/c$ tilasite [$CaMg(AsO_4)F$] and $P2_12_12_1$ adelite [$CaMg(AsO_4)(OH)$], and between $C2/c$ triplite [$Mn_2(PO_4)F$] and $P2_1/c$ triploidite [$Mn_2(PO_4)(OH)$]. Our data on hydroxyl-bästnasite-(Ce) provide another example for an incomplete solid solution arising from the OH-F substitution. Although it appears that the $P\bar{6}2c$ bästnasite-type structure is capable of accommodating a certain amount of OH, as the Raman spectra of most bästnasite-(Ce) and bästnasite-(La) samples in our RRUFF project collection (http://rruff.info) show some weak bands in the OH-stretching region, it is unclear to what extent OH can substitute for F without causing the $P\bar{6}2c$ to $P\bar{6}$ structural transformation,

Akhmanova and Orlova (1966) measured infrared spectra on both bästnasite-(Ce) and hydroxyl-bästnasite-(Ce) and noted that, in addition to the three bands between 3470 and 3620 cm^{-1}, the number of bands in the region of CO_3 symmetrical vibrations for hydroxyl-bästnasite-(Ce) is much greater than that predicted by the selection rules based on the structural symmetry for bästnasite-(Ce). Their interpretation was that the incorporation of OH into the bästnasite structure resulted in a change in the local symmetry of the CO_3 ions, with one group having local symmetry $C3$ and the other $C1$, giving rise to the splitting of the absorption bands for the CO_3 symmetrical vibrations in hydroxyl-bästnasite-(Ce). Apparently, the structure model we report here for hydroxyl-bästnasite-(Ce) offers a better explanation for the observations made by Akhmanova and Orlova (1966) on their hydroxyl-bästnasite-(Ce). Interestingly, although natural hydroxyl-bästnasite-(Nd) with the composition $(Nd_{0.41}La_{0.36}Pr_{0.11}Sm_{0.06}Gd_{0.02}Eu_{0.02}Ca_{0.01})_{\Sigma 0.99}(CO_3)_{1.03}[(OH)_{0.55}F_{0.38}]_{\Sigma 0.93}$ was described to be isomorphous with bästnasite-(Ce) from the X-ray powder diffraction data, its infrared spectrum was more compatible with that reported by Akhmanova and Orlova (1966) for their hydroxyl-bästnasite-(Ce) (Maksimović and Pantó 1985). This observation, together with the $P\bar{6}$ structure of synthetic $NdCO_3(OH)$ (Christensen 1973), leads us to conclude that natural hydroxyl-bästnasite-(Nd) is actually isostructural with hydroxyl-bästnasite-(Ce), rather than with bästnasite-(Ce). A re-indexing of X-ray powder diffraction data for hydroxyl-bästnasite-(Nd) (Maksimović and Pantó 1985) based on the hydroxyl-bästnasite-(Ce) structure yielded a = 12.455(2) (i.e., $\sqrt{3} \times 7.191$), c = 9.921(2) Å, and V = 1332.9 $Å^3$ (i.e., 3×444.3).

Acknowledgments

We gratefully acknowledge the support of this study from the RRUFF project. The electron microprobe analysis was conducted by G. Costin.

References cited

Akhmanova, M.V. and Orlova, L.P. (1966) Investigation of rare-earth carbonates by infra-red spectroscopy. Geochemistry International, 3, 444–451.

Brown, I.D. (1996) Valence: A program for calculating bond valence. Journal of Applied Crystallography, 29, 479–480.

Bünzli, J.-C.G., Comby, S., Chauvin, A.-S., and Vandevyver, C.D.B. (2007) New opportunities for lanthanide luminescence. Journal of Rare Earths, 25, 257–274.

Chi, R., Zhang, X., Zhu, G., Zhou, Z.A., Wu, Y., Wang, C., and Yu, F. (2004) Recovery of rare earth from bästnasite by ammonium chloride roasting with fluorine deactivation. Minerals Engineering, 17, 1037–1043.

Christensen, N. (1973) Hydrothermal preparation of rare earth hydroxycarbonates. The crystal structure of $NdOHCO_3$. Acta Chemica Scandinavica, 27, 2973–2982.

Cooper, M.A. and Hawthorne, F.C. (1995) The crystal structure of maxwellite. Neues Jahrbuch für mineralogie-monatshefte, 3, 97–104.

Donnay, G. and Donnay, J.D.H. (1953) The crystallography of bästnasite, parisite, roentgenite, and synchysite. American Mineralogist, 38, 932–963.

Groat, L.A., Rausepp, M., Hawthorne, F.C., Ercit, T.S., Sherriff, B.L., and Hartman, J.S. (1990) The amblygonite-montebrasite series: Characterization by single-crystal structure refinement, infrared spectroscopy, and multinuclear MAS-NMR spectroscopy. American Mineralogist, 75, 992–1008.

Kirillov, A.S. (1964) Hydroxyl bästnasite, a new variety of bästnasite. Doklady Akademii Nauk SSSR, Earth Science Sections, 159, 93–95.

Kutlu, I. and Meyer, G. (1999) Basische Carbonate des Dysprosiums: $Dy_2O_2(CO_3)$ und $Dy(OH)(CO_3)$. Zeitschrift fuer Anorganische und Allgemeine Chemie, 625, 402–406.

Libowitzky, E. (1999) Correlation of O-H stretching frequencies and O-H···O hydrogen bond lengths in minerals. Monatshefte für Chemie 130, 1047–1059.

Maksimović, Z. and Pantó, G. (1985) Hydroxyl-bästnasite-(Nd), a new mineral from Montenegro, Yugoslavia. Mineralogical Magazine, 49, 717–720.

Mi, J., Shen, J., Pan, B., and Liang, J. (1996) Crystal structure refinement of bästnasite-(Ce) and fluocerite-(Ce). Earth Science—Journal of China University of Geosciences, 21, 63–67. (Chinese with English abstract).

Minakawa, T., Adachi, T., and Matsuda, M. (1992) The first occurrence of hydroxyl-bästnasite in Japan. Chigaku Kenkyu, 41, 155–159 (in Japanese).

Nakamoto, K., Margoshes, M., and Rundle, R.E. (1955) Stretching frequencies as a function of distances in hydrogen bonds. Journal of American Chemical Society, 77, 6480–6486.

Ni, Y., Hughes, J.M., and Mariano, A.N. (1993) The atomic arrangement of bästnasite-(Ce), $Ce(CO_3)F$, and structural elements of synchysite-(Ce), röntgenite-(Ce), and parisite-(Ce). American Mineralogist, 78, 415–418.

Ni, Y., Post, J.E., and Hughes, J.M. (2000) The crystal structure of parisite-(Ce), $Ce_2CaF_2(CO_3)_3$. American Mineralogist, 85, 251–258.

Novak, A. (1974) Hydrogen bonding in solids. Correlation of spectroscopic and crystallographic data. Structure and Bonding, 18, 177–216.

Oftedal, I. (1931) Zur kristallstruktur von bastnäsit (Ce,La--)FCO_3. Zeitschrift für Kristallographie, 78, 462–469.

Sheldrick, G.M. (1997). SHELXS97 and SHELXL97. University of Göttingen, Germany.

Terada, Y., Nakai, I., and Kawashima, T. (1993) Crystal structure of bästnasite (Ce,La,Nd,Sm,Gd)CO_3F. Analytical Sciences, 9, 561–562.

Yang, H., Zwick, J., Downs, R.T., and Costin, G. (2007a). Isokite, $CaMg(PO_4)F$, isostructural with titanite. Acta Crystallographica, C63, i89–i90.

Yang, H., Sano, J.L., Eichler, C., Downs, R.T., and Costin, G. (2007b) Iranite, $CuPb_{10}(CrO_4)_6(SiO_4)_2(OH)_2$, isomorphous with hemihedrite. Acta Crystallographica, C63, i122–i124.

Manuscript received October 17, 2007
Manuscript accepted November 8, 2007
Manuscript handled by Bryan Chakoumakos